Compressed Sensing for Magnetic Resonance Image Reconstruction

Angshul Majumdar

CAMBRIDGE
UNIVERSITY PRESS

CAMBRIDGE
UNIVERSITY PRESS

4843/24, 2nd Floor, Ansari Road, Daryaganj, Delhi - 110002, India

Cambridge University Press is part of the University of Cambridge.

It furthers the University's mission by disseminating knowledge in the pursuit of
education, learning and research at the highest international levels of excellence.

www.cambridge.org
Information on this title: www.cambridge.org/9781107103764

First published 2015

Printed in India

A catalogue record for this publication is available from the British Library

Library of Congress Cataloging-in-Publication Data
Majumdar, Angshul, author.
Compressed sensing for magnetic resonance image reconstruction/Angshul Majumdar.
p. ; cm.
Includes bibliographical references and index.
Summary: "Discusses different ways to use existing mathematical techniques to solve compressed sensing problems"--Provided by publisher.
ISBN 978-1-107-10376-4 (hardback)
I. Title.
[DNLM: 1. Image Processing, Computer-Assisted--methods. 2. Magnetic Resonance Imaging--methods. 3. Algorithms. 4. Models, Theoretical. WN 185]
RC386.6.M34
616.07'548--dc23
2015003684

ISBN 978-1-107-10376-4 Hardback

Contents

List of Figures *vii*
List of Tables *xi*
Foreword *xiii*
Preface *xiv*
Acknowledgements *xvi*
Color Plates *xvii*

1. Mathematical Techniques

1.1 Compressed Sensing 3
1.1.1 Sparse Recovery 3
1.1.2 Group-sparse Recovery 7
1.1.3 Row-sparse Multiple Measurement Vector Recovery 8
1.1.4 Synthesis and Analysis Priors 9
1.2 Low-rank Matrix Recovery 10
1.3 Kalman Filter 13
1.4 Algorithms 15
1.4.1 Noiseless Scenario 15
1.4.2 Noisy Scenario 21
1.5 Split Bregman Techniques 30
1.5.1 Multiple Penalty Problems 34
1.6 Conclusion 37
Appendix: Greedy Algorithms 38
References 44

2. Single Channel Static MR Image Reconstruction

2.1 Single Echo MRI Reconstruction 50
2.1.1 Sparsity 52
2.1.2 Incoherence 55
2.1.3 Reconstruction Algorithms 58
2.1.4 Engineering the Measurement Operator 62
2.1.5 Structured Sparsity 65
2.2 Multi-echo MRI 72
2.2.1 Physics of MR Image Contrast 73
2.2.2 Group-Sparse Reconstruction of Multi-echo MRI 75
Appendix: Mixed Prior Optimization 81
References 84

3. Multi-Coil Parallel MRI Reconstruction

3.1 Frequency Domain Methods 87
3.1.1 GRAPPA 88
3.1.2 Regularized GRAPPA 89
3.1.3 Iterative GRAPPA 90
3.1.4 Kernel GRAPPA 92
3.1.5 Extensions to GRAPPA 94
3.2 Image Domain Methods 98
3.2.1 SENSitivity Encoding 99
3.2.2 Regularized SENSE 100
3.2.3 CS SENSE 103
3.2.4 Iterative SENSE 104
3.3 Calibration-Free Reconstruction 107
3.3.1 Calibration-Less Multi-coil MRI 109
3.4 Conclusion 116
References 117

4. Dynamic MRI Reconstruction

4.1 Offline Dynamic MRI Reconstruction 121
4.1.1 Compressed Sensing-Based Reconstruction Techniques 121
4.1.2 Low-Rank Methods in Dynamic MRI Reconstruction 125
4.1.3 Combined Low-Rank and Sparsity-Based Techniques 127
4.1.4 Sparse + Low-Rank Reconstruction 137

4.2 Online Reconstruction 140
4.2.1 Compressed Sensing-Based Techniques 140
4.2.2 Kalman Filter-Based Techniques 146
4.2.3 Hybrid Methods 149
4.3 Dynamic Parallel MRI 153
4.3.1 Image Domain Methods 153
4.4 Conclusion 156
References 157

5. Applications in Other Areas

5.1 Computer Tomography 160
5.1.1 Compressed Sensing in Static CT Reconstruction 162
5.1.2 Compressed Sensing in Dynamic CT 167
5.2 Diffusion Tensor Imaging 172
5.2.1 Distributed Compressed Sensing 173
5.2.2 Learned Dictionary Approach 174
5.2.3 Direct Diffusivity Estimation 175
5.3 Compressed Sensing in EEG Reconstruction 177
5.3.1 Improving Transmission Energy Efficiency by Compressed Sensing 177
5.3.2 Improving Sensing Energy Efficiency 184
5.4 Conclusion 189
References 190

6. Some Open Problems

6.1 Interactive Sampling 194
6.1.1 Recursive Least Squares 197
6.1.2 Recursive l_1-Filtering 198
6.1.3 Discussion 201
6.2 Quantitative MRI 201
6.2.1 Non-linear Compressed Sensing Recovery 202
6.3 Parallelizing MRI Reconstruction Algorithms 204
References 205

Index *207*
About the author *208*

Cambridge University Press
978-1-107-10376-4 - Compressed Sensing for Magnetic Resonance Image Reconstruction
Angshul Majumdar
Frontmatter
More information

List of Figures

1.1 Geometry of l_1-norm minimization. 5

1.2 Kalman filter. 14

1.3 Majorization–minimization [50]. 22

2.1 Left to right: brain image, horizontal gradient, vertical gradient. 52

2.2 Wavelet decomposition of brain image. 53

2.3 Decay of coefficients in the transform domains. 54

2.4 Decay of unnormalized coefficients in the transform domains. 54

2.5 Example on Restricted Isometric Property. 55

2.6 Multiple-slit experiment (modification from Feynman's thought experiment). 57

2.7 Reconstructed and Difference Images 63

2.8 Sampling patterns: random lines, Gaussian and radial (non-Cartesian). 64

2.9 Hierarchical correlation. 66

2.10 Tree structure. 67

2.11 Left to right: Spine (rat), brain and phantom. 71

2.12 Reconstructed and difference images. Left to right: sparse recovery, tree-sparse recovery, synthesis prior elastic net, and analysis prior elastic net. 72

2.13 Images of same cross section of brain with different T_2 weightings (courtesy Piotr Kozlowski). 76

2.14 First T_2 weighting: (2a) tissue boundary; (2b) wavelet coefficients. 77

2.15 Second T_2 weighting: (2a) tissue boundary; (2b) wavelet coefficients. 77

2.16 Scatter plot of wavelet coefficients of two T_2 weighted images of rat's spinal cord. 78

2.17 Grouping of wavelet coefficients according to their position. 78

2.18 Top row – ground-truth images. Next three rows – piecemeal reconstruction via CS, group-sparse synthesis prior, and group-sparse analysis prior reconstruction. 80

3.1 Images from different coils. 87

3.2 Comparative reconstruction results [17]. 90

3.3 Reconstructed images. From left to right: fully sampled, GRAPPA reconstruction and iGRAPPA reconstruction [19, 20]. 92

3.4 Comparison of reconstruction results from GRAPPA and variants [25]. 95

3.5 (a) GRAPPA reconstruction and (b) SPIRiT reconstruction [9]. 96

3.6 GRAPPA and L_1-SPIRiT reconstruction of abdomen scan [9]. 97

3.7 A water phantom. Top – reconstructed images and bottom – difference images. Left – SC GRAPPA and right – GRAPPA [10]. 99

3.8 The reconstructions using four different methods with reduction factor 4 from an 8-channel scanned human brain data [30]. 102

3.9 Left to right: CS SENSE reconstructed image, CS SENSE difference image, NNSENSE reconstructed image, and NNSENSE difference image. 103

3.10 Top row: Sensitivity maps; bottom row: decay of singular values. 106

3.11 iSENSE reconstructed images in each step. 107

3.12 (a) Sharp edge and (b) less prominent edge 110

3.13 (a) Finite differencing of sharp edge and (b) finite differencing of less prominent edge 111

3.14 Reconstructed images from various methods. From top to bottom: GRAPPA, CS SENSE, CaLM synthesis prior, CaLM analysis prior. 113

3.15 Brain images from 8-channel scanner. 114

3.16 Decay of singular values. 115

3.17 Reconstructed (top) and difference images (bottom) – Left to right: SparSENSE, L_1-SPIRiT, CaLM, and low-rank CaLM. 115

4.1 Reconstructed and difference frames. 123

4.2 Reconstructed images. Top to bottom: Ground-truth, temporal TV [5] reconstruction, and sliding window reconstruction. 124

4.3 Reconstructed (Top row) and difference images (bottom row). From left to right – Ground-truth, temporal TV [5], and Spatiotemporal TV [6]. 126

4.4 Reconstructed images by low-rank techniques [13]. 127

4.5 (a) Low-rank reconstruction, (b) CS reconstruction, and (c) combined low-rank and CS reconstruction. Top row – reconstructed images and bottom row – difference images [15]. 128

4.6 Reconstruction from low-rank penalty, sparse penalty, and combined low-rank and sparse penalty [16]. 130

4.7 From left to right: Ground-truth, reconstruction from [15] and reconstruction from [17]. 131

4.8 Left to right: ground-truth, zero-filling, compressed sensing (assuming sparsity in *x-f* space), and BCS [20]. 132

4.9 Reconstructed images. Top – 2D DCE1; bottom – 2D DCE2; left to right – ground-truth, k-t SLR, sBCS, sBCS LR, and aBCS LR. 136

4.10 Difference images. Top – 2D DCE1; bottom – 2D DCE2; left to right – ground-truth, k-t SLR, sBCS, sBCS LR, and aBCS LR. 137

4.11 (from [21]). L + S decomposition of fully sampled 2D cardiac cine (a) and perfusion (b) datasets corresponding to the central x location. 139

4.12 (from [21]). Systolic phase images and x-t plots (in panels to the right of the short-axis images) corresponding to the reconstruction of cardiac cine data with simulated acceleration factors R = 4, 6, and 8 using compressed sensing (CS), simultaneous low-rank and sparsity constraints (L&S) and L+S decomposition (L+S). 140

4.13 Reconstructed images using various techniques. 142

4.14 Top: Three consecutive images from a larynx sequence; bottom: difference images between the three consecutive frames. 143

4.15 Top: Sorted pixel values of the difference images; bottom: sorted wavelet coefficients of the difference image. 144

4.16 Left to right: ground-truth, CS reconstruction [30], LS-CS and Kalman filter. Top – reconstructed images; bottom – difference images. 146

4.17 Normalized absolute autocorrelation function estimate of the difference between two cardiac images. 147

4.18 Reconstruction of three consecutive frames. 148

4.19 (a) Difference between previous and current frame; (b) difference between predicted and current frame; (c) sorted coefficients. 151

4.20 Schematic diagram for prediction and correction steps. 152

4.21 Reconstructed (top) and difference (bottom) images. Left to right: ground-truth, sliding window, KF, CS reconstruction [30], hybrid. 152

4.22 k-t SENSE sampling patterns. 153

4.23 Comparison of reconstruction results from various methods. 155

4.24 Still from cardiac sequence. Reconstructed and difference images in pairs. L-R: SPEAR, k-t GRAPPA, and k-t CaLM. 156

5.1 Simple X-ray CT [1]. 161

5.2 From top to bottom: Ground-truth, synthesis prior, TV minimization, weighted TV, and constrained TV. 166

5.3 Variation of RMSE with time. 170

5.4 Left to right: Ground-truth, difference image from NCPICCS, reconstructed image from NCPICCS, difference image from proposed method, and reconstructed image from proposed method. 171

5.5 Reconstructed images. (L-R): Ground-truth, NCPICCS, SRM, and low-rank + sparse. 172

5.6 Difference images (Ground-truth – Reconstructed). (L-R): NCPICCS, SRM, and low-rank + sparse. 172

5.7 ODFs for subject A using Wavelet + TV (a), dictionary (b), and fully sampled data (c) within the ROI in the FA map in (d). 175

5.8 Numerical phantom results [37]: (a) Reference ODF reconstructed using 47 angular measurements. (b), (c) ODF reconstructed at acceleration of 4 using q-only and k-q downsampling, respectively. 176

5.9 (a) Synthesis prior Gabor basis with Gaussian compression [13, 18]; (b) synthesis prior Gabor basis with binary compression [16]; (c) Block Sparse Bayesian Learning (BSBL) [19]; (d) joint synthesis prior [21]; (e) analysis prior [23]; (f) joint row-sparse analysis prior [24]. 185

5.10 Decay of Fourier coefficients for a single EEG signal. 187

5.11 Decay of Fourier coefficients for EEG signal ensemble. 187

5.12 Decay of singular values for multichannel signal ensemble. 188

6.1 The top row shows brain images reconstructed from radial sampling. From left to right, the number of radial spokes used is 12, 25, 37, 50, and 62. The bottom row shows reconstructed heart images with 12, 25, and 37 radial spokes. 195

6.2 Brain and cardiac MR images. Top – wavelet coefficients; bottom – decay of wavelet coefficients. 196

List of Tables

2.1 Reconstruction results 71
3.1 GRAPPA reconstruction 108
3.2 CS SENSE reconstruction 108
3.3 Coil correlations (since the full table will be symmetric, only the upper half is shown) 114
3.4 Reconstruction accuracy in NMSE 116
4.1 NMSE for various techniques 135
4.2 Relative mean squared error and structural similarity index values [21] 139
4.3 Reconstruction times (in seconds) for different methods 153
5.1 NMSE for different number of projections 165
5.2 Comparative reconstruction accuracy 172
5.3 Root-mean-square error (RMSE) of fractional anisotropy (FA), mean diffusivity (MD), and angular deviation of the primary eigenvector ($\Delta\alpha$) estimated from DCS-based reconstructions at varied acceleration factors (R) 174
5.4 Evaluation of reconstruction techniques 184
5.5 Comparative reconstruction results (NMSE) 189

Foreword

This is a much needed book that skilfully discusses the fascinating subject of MRI reconstruction procedures and its applications. Many research developments in the area of MRI reconstruction took place in the late 1990s and early 2000s. But it was not until 2006–07 that researchers showed how to harness powerful techniques developed in applied mathematics and theoretical signal processing to accelerate MRI acquisition. This generated lots of enthusiasm in MRI reconstruction research, a branch popularly known as 'Compressed Sensing'. There are several books on MRI, covering aspects like MR physics or its clinical applications or covering both aspects. But only a few amongst them cover, in an exhaustive manner, topics on MR image formation and analysis or 'MR reconstruction' as it is more popularly called. Prior to the application of Compressed Sensing in MRI, the literature on MRI reconstruction procedures could be covered in a chapter or two. But in the post Compressed Sensing era, a plethora of new mathematical techniques and algorithms are being applied for MRI reconstruction procedures and hundreds of research papers have appeared on this topic. This emphasizes the need for a comprehensive book that deals with the various aspects of Compressed Sensing in MRI.

This book organizes all the modern MRI reconstruction techniques in a clear and concise manner and one can easily sense the practical experience of the author in this area. Compressed Sensing, being a highly mathematical topic, requires graduate level training in applied mathematics. However, this book keeps the theory of Compressed Sensing to a minimum without diluting the fundamental concepts and it introduces it in an intuitive fashion. Anyone with a basic degree in science and engineering can easily follow this book. Thus, the scope of this book stretches from the fundamentals of mathematical theory to the most advanced MRI reconstruction procedures and algorithms and their applications in MRI.

I am convinced that this book will serve as an excellent source of information for senior undergraduate as well as graduate students. Further, it may also be used by educationalists who want to design a full course on MRI reconstruction. Researchers in signal processing who want to learn about the applications of mathematical techniques in MRI reconstruction or medical physicists who would like to be abreast with the latest in MRI reconstruction will also find this book to be an excellent reference.

Professor N. R. Jagannathan
Department of NMR & MRI Facility
All India Institute of Medical Sciences, New Delhi

Preface

This book is about modern approaches to magnetic resonance imaging (MRI) reconstruction. In the last decade, MRI has benefitted immensely from advances in applied mathematics and signal processing. Leveraging these techniques, MRI scans are now being performed two to four times faster than before. In this book, we learn how these techniques have been used in the recent past to accelerate MRI scans.

During my PhD, I worked on a few different areas of MRI reconstruction – static MRI, dynamic MRI, parallel MRI (static and dynamic) and quantitative MRI. After I relocated to India, Manish Chaudhury commissioning editor at Cambridge University Press, inspired me to write a book and I was eager to write about signal processing techniques in MRI. It took me about one and half years to complete this volume.

When I started working on MRI reconstruction, I felt that there is a gap between the practitioners and the theoreticians. On one side, there were researchers in signal processing and applied maths who were interested in theoretical proofs and algorithms. On the other, there were the MRI physicists and engineers who had lots of interesting problems that were waiting to be solved. Since then, many researchers have worked very hard to reduce this gap. The concerted effort of so many researchers is finally bearing fruit; in the past few ISMRMs, MRI scanner manufacturers showed interest in adopting these advanced signal processing techniques for image reconstruction.

In this book, I have made every effort to incorporate interesting studies on MRI reconstruction, but I may have missed out a few unintentionally. Thus, this book does not claim to be an encyclopaedic review on the subject of signal processing techniques in MRI reconstruction.

The targeted audience of the book are signal processing engineers who want to learn about MRI problems and MRI physicists who want to know how signal processing is benefitting MRI. The book can also be perused by doctors who have a background in mathematics. I do not presume a reader who has an advanced background in mathematics. But the reader is expected to have some undergraduate training in linear algebra, probability and convex optimization. Otherwise, the book may not be easy to follow.

The book starts with an introduction on all the mathematical techniques one needs to know to understand the subsequent chapters. The emphasis of the first chapter is on algorithms. There are no proofs; rather, the reader is walked through the essence of the theoretical results based on mathematical intuitions. The second chapter is on single-channel static MRI reconstruction. Clinically, this is perhaps the most widely used modality. The third chapter talks about multi-coil parallel MRI. This is a very interesting topic; it is the perfect example of how signal processing (mathematical)-based acceleration techniques can be combined with hardware (physics)-based methods to reduce scan times. The fourth chapter is on dynamic MRI reconstruction. In the fifth chapter, we digress from the main theme of the book; we discuss how signal processing techniques have benefited other areas in biomedical engineering. The final chapter is a short one. It confines itself to some open problems in signal processing-based MRI reconstruction. Although each chapter is fairly independent, I advise the reader to go through them sequentially.

Acknowledgements

About a third of the contents of this book were techniques developed during my PhD. Usually a PhD focuses on a single topic. But Dr Rabab Ward, my supervisor, gave me the freedom and flexibility to choose and work on any problem I liked. In addition to exploring various topics of MRI, I also worked on color imaging, sensor networks and certain aspects of machine learning. I am thankful to her for her care and support that extended beyond academics.

I am indebted to Dr Felix Herrmann of UBC for introducing me to the topic called Compressed Sensing. It happened during my first year as a graduate student in the Fall of 2007. Compressed Sensing is a complex mathematical topic, but Felix explained the subject in a fashion that I could easily grasp without much background in mathematics. He interpreted the mathematical results in a very intuitive and interesting fashion. Throughout the book, I have tried to follow Felix's philosophy of explaining complex mathematics in an easy to understand way.

Finally, I would like to thank Dr Pankaj Jalote, who is the founder director of IIITD. He made the transition of young faculty members from other countries to India extremely smooth. I felt comfortably settled in my office within a fortnight of joining the institute. This has helped, immensely, in writing this book.

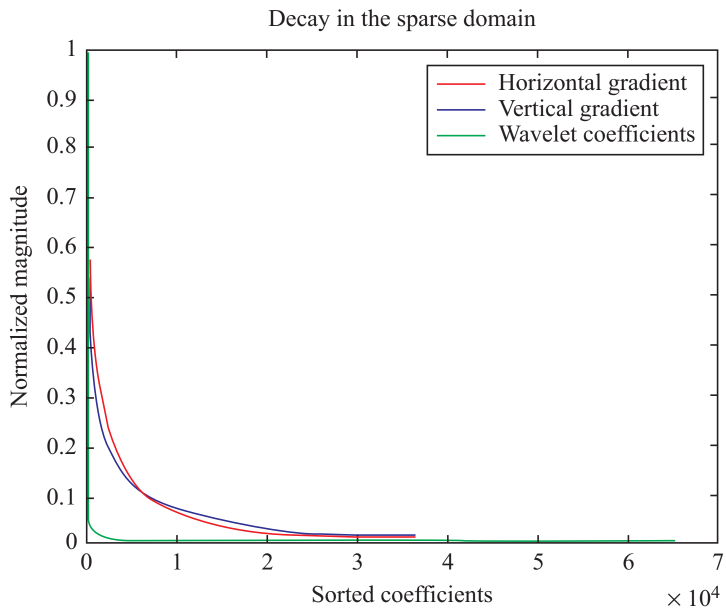

Figure 2.3 Decay of coefficients in the transform domains [see page 54].

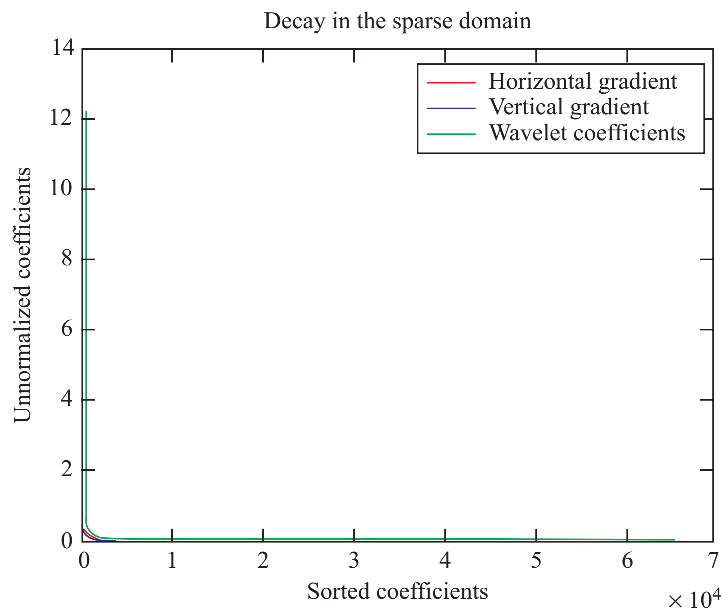

Figure 2.4 Decay of coefficients in the transform domains [see page 54].

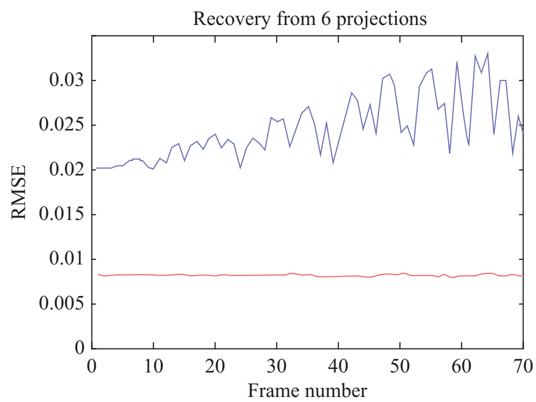

Figure 5.3 Variation of RMSE with time. Blue plot represents error from NCPICCS and red plot represents error from low-rank recovery method [see page 170].

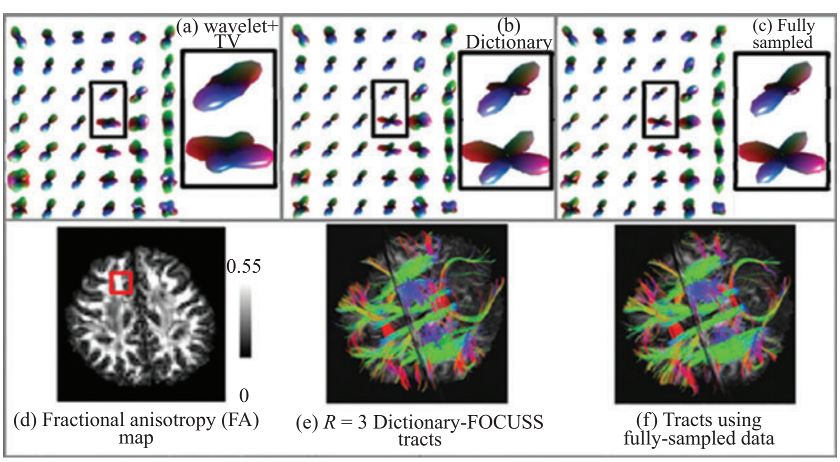

Figure 5.7 ODFs for subject A using Wavelet + TV (a), dictionary (b), and fully sampled data (c) within the ROI in the FA map in (d). Tracts with $R = 3$ dictionary recon (e) and fully sampled data (f) are also presented [see page 175].

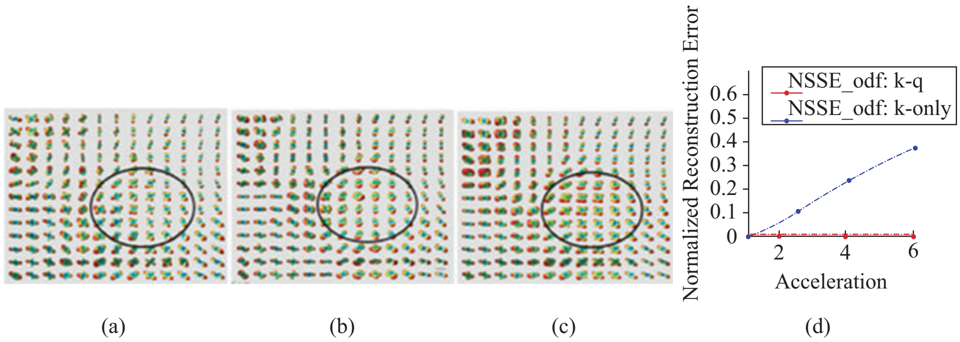

Figure 5.8 Numerical phantom results [37]: (a) Reference ODF reconstructed using 47 angular measurements. (b), (c) ODF reconstructed at acceleration of 4 using q-only and k-q downsampling, respectively [see page 176].